Seismic Attenuation and Active Tectonics in Alaska

A THESIS

SUBMITTED TO THE FACULTY OF

UNIVERSITY OF MINNESOTA

BY

Ozan Karayazi

IN PARTIAL FULFILLMENT IF THE REQUIREMENTS

FOR THE DEGREE OF

MASTER OF SCIENCE

Maximiliano Bezada

June, 2022

Acknowledgements

This work would not have been completed without the EarthScope Transportable Array data, thank you for the great work of those who make it possible to observe seismic data.

Furthermore, I would like to thank to my supervisor, Dr. Maximiliano Bezada for your continuous support, professional guidance, and patience. His support motivated me to go further and improved the thesis to a higher level. Next, I would like to thank committee members Prof. Donna Whitney and Prof. Justin Revenaugh who spared time and effort to read this thesis. I would like to thank the Education Ministry of Turkey for financial support and Dr. Selim Ozalp for his mentoring.

Last but not least, I would like to thank my wife, friends and family for always supporting me during this research and my entire study.

Abstract

Using deep teleseismic earthquakes recorded by the EarthScope Transportable Array and other temporary broadband deployments, we map the attenuation below Alaska. We measure 209 events that passed our quality control test using a time-domain approach to measure P wave attenuation. Our results show a good correlation with attenuation being dominated by sub-crustal structure and with expectations from the velocity-defined lithospheric domains. High-attenuation regions generally exhibit quaternary volcanic fields and arc and back-arc regions, which surprisingly show more attenuation than previous studies, highlighting the need for a better understanding of the effect of melt and volatile contents in mantle attenuation. Low-attenuation regions include an undeformed, seismically inactive region north of the Brooks Mountains. In addition, the remaining slab of the subduction zone from the interior of the continent also shows low attenuation. Comparisons made with additional features such as intra-continental deformation, magmatism, and seismicity contribute to our study.

Table of Contents

List of Figures

1. Introduction

The constitution of the Earth, its current structure, and its character are very important to scientists of varying fields. Earth sciences contribute not only to a better understanding of the formation and development of the Earth but also people's lives. For example, a development in Earth sciences can also contribute to the location selection of structures or determining the properties of buildings in civil engineering. In addition, together with the information concerning the development processes of the Earth, it is possible to obtain information about the past and current processes of the Earth's climate, and then produce predictions for the future. The magnitude and frequency of earthquakes pose a danger to people and the infrastructure of the region. Especially in seismically active regions, precautions taken against hazards are important (Koehler, Carver, and Alaska Seismic Hazards Safety Commission 2018). Seismicity, which is tectonic activity, is defined by Gutenberg and Richter (1941) as a measure that covers earthquake occurrences, mechanisms, and magnitude in a particular region or the world. Many tectonic activities occur at plate boundaries or nearby. For intraplate deformation to occur, the forces applied at the plate boundary are transmitted over long distances, affecting the stress within the plate and causing intraplate deformation (Tommasi, Vauchez, and Neves 2009). The understanding of not only the Earth's surface but also its subterranean layers has gained a lot of importance with the development of technology in recent years. Not only geologically, but also geophysically—thanks to the deployment of larger numbers of instruments, especially in recent years—great progress has been made. In this way, the analysis techniques, methods, and data produced in

Earth sciences have become much more accessible and developable, thanks to the increase in the number of devices, the ease of access to them, and the development of computer systems.

If the Earth behaved in a completely elastic manner, seismic waves could propagate indefinitely. However, the Earth does not act with complete elasticity. For this reason, attenuation occurs during the propagation of seismic waves. According to Shearer (2009), the transformation of energy into heat or loss of energy against internal friction during the passage of a weakening elastic wave constitutes attenuation. In addition, due to this energy loss of the wave, its amplitude also decreases over time.

Generally, the seismic waves created by the energy released by earthquakes lose amplitude from the earthquake source by the time they reach the recording station. This can be due to factors such as geometric spreading and energy portioning at interfaces. Energy loss, which is defined as attenuation, develops as a result of the anelastic behavior of subsurface materials, apart from these factors. Therefore, it must be cleared from other energy-losing factors for attenuation detection.

In seismology, attenuation measurements are made using P and S waves, and surface waves. In addition, laboratory measurements can be made from rock samples according to the changing pressure, temperature, and saturation conditions in laboratory observations (Byrnes and Bezada 2020). There are two essential purposes for conducting attenuation studies. The first purpose is regarding the attenuation of amplitudes of seismic waves from subsurface material and investigating the dependence of this damping on its frequency. Secondly, it is the desire to obtain information about the

lithology and physical conditions of the rocks in the areas that cause attenuation. Attenuation, which is the result of the anelastic behavior of subsurface materials, is a concept that contradicts some theoretical perspectives but does not contradict wave propagation theory. Although wave propagation in an elastic environment is very well understood, limited information is known about the mechanisms that produce anelasticity in mantle rocks. The reason for this is the changes in the physical conditions of the materials that make up the rocks, and therefore this complexity cannot be explained by a single model or mechanism (Tisato, Madonna, and Saenger 2021).

The EarthScope Transportable Array project has created an extraordinary opportunity for the Earth sciences. After this project, funded by the National Science Foundation, it was possible to conduct many studies on the American mainland and Alaska. Thanks to this project, many resources have been provided for seismic studies with the data obtained from the thousands of stations established. In addition, much work has been produced in recent years on seismic velocity tomography in the Americas and Alaska (e.g., Schmandt and Lin 2014; Nayak et al. 2020; Skarlatoudis, Thio, and Somerville 2022; Jiang et al. 2018; Gama et al. 2021; Lanza et al. 2020).

The fact that Alaska, and especially the southern region of Alaska, is one of the most active seismic regions in the world (Koehler, Carver, and Alaska Seismic Hazards Safety Commission 2018), the data accessibility provided by the Earthscope project, and that attenuation is still very debatable, encouraged us to work in this region. In this study, we mapped Alaska's attenuation using the Earthscope Transportable array and temporary

deployments. As a result of these analyses, we studied the relationship between attenuation and volcanic activity, deformation, and the subduction zone in Alaska. These observations are compared with other attenuation studies to evaluate our results.

1.1. Geology Of Alaska

Seismicity in Alaska is mainly controlled by the subduction of the Pacific plate under the North American plate. The stresses caused by this plate convergence are transmitted into (from south to north) Alaska at distances greater than 800 km. In addition, deformation in the interior of Alaska results in crustal seismicity (Ratchkovski 2002). Moreover, plate boundary deformation is dominant in these regions (Tian and Zhao 2012). In the northern slope of Alaska, intracontinental deformation is dominant as well. There are two important simultaneous events in the history of this region: the opening of the Arctic Ocean, and the rise of the Brooks Mountains (Coakley and Watts 1991).

1.1.1. Terranes and Composite Terranes

In tectonic reconstructions, larger terranes in Alaska are grouped into composite terranes (CT) depending on affinities in their inferred litho-tectonic unit and tectonic evolution. These are Arctic CT, Central CT, Yukon CT, Wrangelia CT, Southern Margin CT, and Yakutat terrane (Plafker and Berg 1994). The Arctic terrane, which is in the north of Alaska, comprises about 25% of the total area of Alaska terranes. The Arctic CT includes the Arctic Alaska Terrane and its subterranes. The stratigraphy of the Arctic CT is characterized by deformed Late Proterozoic to Devonian rocks showing

continental margin and carbonate platform sedimentation, settling of Late Proterozoic and Cambrian tholeiitic basalt, and eruption of andesitic Ordovician volcanic rocks (Plafker and Berg 1994). The Central composite terrane, which is located in central Alaska between the Denali and Tintina-Kultag Faults, makes up 7% of the Alaskan area between the Brooks and Alaska ranges. This terrane contains large areas of discontinues so relationships between units are not very well known (Plafker and Berg 1994). The Yukon composite terrane comprises 10% of the area of Alaskan terranes. The Yukon CT consists of crystalline rocks and overlying arc-related rocks in east-central and southeastern Alaska (Plafker and Berg 1994). The Wrangellia CT constitutes about 20% of the area of the Alaskan terranes and occurs between the Denali and Border Ranges fault systems. It is characterized by Late Proterozoic and younger magmatic arc, oceanic plateau and rift fill aggregation, and the Late Jurassic to mid-Cretaceous magmatic arc and flysch deposits of the Gravina-Nutzotin belt (Plafker and Berg 1994). The Southern Margin composite terrane constitutes about 20% of the area of Alaskan terranes. It includes the Chugach, Ghost Rocks, and Prince William terranes. The Southern Margin CT is a compound, deformed accretionary prism of Upper Triassic to Paleogene oceanic rocks, melange, and flysch (Plafker and Berg 1994). The Yakutat terrane makes up 5% of all terranes in Alaska. The Yakutat terrane is an allochthonous fragment of the continental margin. It has a basement of Paleocene and Eocene oceanic crust in the western part and a part of the Southern Margin composite terrane in the eastern part (Plafker and Berg 1994).

1.1.2. Faults in Alaska

One of the most important factors controlling tectonism in Alaska is faults. The Denali Fault is a continental right-lateral strike-slip fault extending from western North America to central Alaska, and it is over 2000 km long (Fig 1). Faults in Alaska are the result of tectonic activity under the control of the subduction zone between the south Pacific Plate and the North American plate. The Denali fault, located on the border between two plates, has a displacement rate of 1mm to 35mm per year. In addition, the Denali fault is one of the structures that provide compression and stress control in Central Alaska (Eberhart-Phillips et al. 2003; Plafker and Berg 1994). The Tintina fault is a right-lateral strike-slip fault, approximately 1000 km in length, extending from western North America to central Alaska. It represents the Yukon continuum between the Rocky Mountain Trench in North America and the Kaltag Fault in Alaska, as well as having an impact on tectonic activity in southwestern Alaska. The Kaltag fault is a 500 km long right-lateral strike-slip fault. This fault, which starts in central Alaska and extends to western Alaska, has an active role in the tectonics of central and western Alaska (Plafker and Berg 1994).

1.1.3. Mountain Ranges in Alaska

Alaska has fourteen mountain ranges. The three major ranges are the Alaskan Mountain Range, the Brooks Range, and the Aleutian Range (Fig 1). The Alaska Mountain Range, which is 600 miles in length, stretches from Lake Clark (154˚W) in the southwest to the Yukon Territory in the southeast, located in south-central Alaska. It also contains the highest mountain in North America, Mount Denali. The Brooks Range are mountain ranges in northern

Alaska that are about 700 miles long, stretching from west to east from Alaska to the Yukon region. The highest peak in this mountain range is Mount Isto. The Aleutian Range is a 600-mile-long mountain range in southwestern Alaska that stretches from Lake Chakachamna (152˚W) to the island of Unimak (164˚W). The greatest feature of this mountain range is that it has a large number of active volcanoes that are part of the Aleutian Arc. It also includes all the mountains of the Alaska Peninsula. Apart from these 3 major mountain ranges, the Ogilvie Mountain, Yukon Tanana Uplands, Wrangell-St. Elias Mountains, St. Elias Mountains, Chugach Mountain, Kenai Mountains, Talkeetna Mountains, Kuskokwim Mountains, Nulato Hills, and Seward Peninsula Mountains are the other mountain ranges in Alaska.

2. Data And Method

2.1. Data Selection

In this study, seismic waveforms collected in Alaska are used. Waveforms are processed at each station to measure differential body-wave attenuation (Δt*) from teleseismic P waves. A unique data set is provided by the recently expanded broadband distribution in Alaska. We analyze data collected between January 1999 and April 2021 from stations located 43˚to 75˚north and 175˚to 125˚west. The networks used are: TA (2003-continued): USArray Transportable Array (IRIS Transportable Array 2003) and AK (1987-continued): Alaska Regional Network (Alaska Earthquake Center, Univ. of Alaska Fairbanks 1987) (stations with the most dense coverage in Alaska)) stations in addition to XR (2004-2007): CSEDI: Observational and Theoretical Constraints on the Structure and Rotation of the Inner Core (Song and

Christensen 2010), YV (2010-2010): Bering Glacier Surge Seismic Experiment (Waite 2012), XE (1999-2001): Broadband Experiment Across the Alaska Range (Christensen, Hansen, and Abers 1999), XZ (2005-2012): Collaborative Research: St. Elias Erosion/Tectonics Project (Hansen and Pavlis 2005), YG (2016-2018): Fate and consequences of Yakut terrane subduction beneath eastern Alaska and the Wrangell Volcanic Field (Christensen and Abers 2020), ZE (2015-2017): Southern Alaska Lithosphere and Mantle Observation Network (Tape, Christensen, and Moore-Driskell 2019). The combination of these deployments provides high-resolution imaging (Fig 2).

In this case, the time domain waveform modeling approach is used to estimate Δt* (Bezada 2017). Deep events of 250-750 km depth, recorded at stations around Alaska, are used. Also, the magnitudes of these events are limited to greater than 5.7. The reason why we limit depth and magnitude is that deep events are attenuated almost exclusively on the receiver side. The size limitation is due to the fact that waveforms are impulsive and have a sufficiently large signal-to-noise ratio. We also applied more constraints by requiring 30°-90° azimuth distances. Direct P-waves exhibit complex features below 30° and are not present due to the shadow-zone above 90°. A total of 370 events recorded by the stations met our criteria.

2.2. Δt* calculation and creating an attenuation map

The first step toward estimating Δt*, is to find the least attenuated (sharpest P-wave peak observed in traces) record for each event, which is considered as a reference trace. All traces are aligned by finding other unattenuated traces in the data. The waves may differ from the codas after

the primary pulse, but the data selection is not coda sensitive. After all the traces are matched and aligned, the fit window is determined, and the fit waveform is created. A synthetic Δt* is then generated for each trace observed. At this stage, observational checks are made again and the compatibility of synthetic traces and observed traces is checked (Fig 3). If the observed first pulse and synthetic Δt* do not match or the match is poor, it is rejected. In this study, all 370 events were analyzed, and inversion studies were continued with 209 events whose Δt* measurement passed quality control.

During the calculation of Δt*, which is the seismic wave attenuation factor, the uncertainties of the measurements were high due to reasons such as different types of noise, scattering caused by velocity fluctuations, and topographic effects close to the receiver (Gao 1997).

This dissipation of seismic energy is quantified by the parameter Δt*, which represents the inverse of the quality factor integrated over the path:

$$t^* = \int \frac{dt}{Q(t)} = \int \frac{dx}{c(x)Q(x)}$$

Where Q is the quality factor, and c is the seismic wave velocity.

As stated in the previous research (Zhu et al. 2021; Bardsley 2012; Byrnes et al. 2019) the Bayesian Linear Inversion Markov Chain Monte Carlo (MCMC) method was used to map the Δt* calculation at the stations. The Bayesian method based on MCMC allows practical alternatives considering minimal external constrains (Zhu et al. 2021). In MCMC sampling, values are taken from a probability distribution that shows the current value depending on the previously plotted value. In that sense, multiple independent chains are

generated with models which illustrated with arbitrary number of nodes generated Δt* values. The aim of this step is to evaluate the convergence of MCMC chains towards a boundary, it is useful to construct multiple chains with different initial values. These multiple chains are combined to calculate the model summary. The sampling iteration specifies the number of iterations in the sampling phase that can be described as the length of the MCMC chain. The number of samples required to achieve convergence and have sufficient precision depends on the complexity of the data and model. As far as considered Δt* values, each model can be manipulated with these five approaches; to create a new node; to eliminate an existing node; to alternate Δt* values of a node; to shift an existing node to another location; to disturb the vagueness the data (Zhu et al. 2021). In this research, we specified 75 km as the distance between two stations (node spacing). The weighted average parameter is selected with stations within a 100 km radius of each node. Additionally, based on a number of different tests (6 chain 500 iteration, 6 chain 1000 iteration, 12 chain 500 iteration, 12 chain 1000 iteration) (Fig 5), the number of chains is implemented as 12, and the number of times to iterate is selected as 1000.

3. Results

The attenuation map created from the Bayesian inversion over the Δt* measurements is shown in figure 4. The attenuation map shows consistency generally with what we expected. The Subducted slab below the continent shows the lowest attenuation. Other low-attenuation areas includethe Cougach Terrain, a member of the southern margin composite terrain, to

Yukon Composite Terrain, north of the Alaska Mountain Range, St Elias Mountain region southeast of Wrangell Volcanic Field, and the Colville Basin located in the Arctic Composite Terrain in northern Alaska (Δt*= from -0.15 to -0.1 s). The regions where the highest attenuation is observed are; the back-arc and arc region between the northwest of the Cook Inlet Basin and the western segment of the Denali Fault, the west Alaska region between the Seward Peninsula (north) and the Bethel Basin (south), and northeast Alaska, between east of the Brooks Range and the Richardson Mountains (Δt* equal and greater than 0.1 s).

The Alaska Peninsula, located in southwestern Alaska, exhibits moderate attenuation. According to Jiang et al. 2018, the slab is approximately 50-100 km deep along the Alaska Peninsula. It shows lower attenuation because the slab is still relatively cold (Stachnik, Abers, and Christensen 2004) (Δt*=~-0.05 s). In contrast to consistent areas, the higher attenuation in the arc and back-arc region is more than the expected result (Δt*=0.1 s).

In western Alaska, it is consistent to show high attenuation (Δt*=0.04-0.1 s) due to magmatism, with a thin lithosphere, deformed by the compression of the Bering plate and the pacific plate. (Gama et al. 2021)

Central Alaska, one of the most seismically active regions of North America (Dixit and Hanks 2021), shows moderate seismic attenuation. Although this strong continental plate has intracontinental seismicity and earthquakes, it is consistent to show moderate attenuation due to tectonic

forces and stresses in the region hundreds of kilometers from the subduction zone (Dixit and Hanks 2021).

We note that the lowest seismic attenuation in the Colville Basin correlates with and almost seismically inactive region north of the Brooks Range. The high attenuation area seen in northeast Alaska is correlated with Quaternary volcanism (Richardson Mountains). The boundaries between intra-continental seismicity and high-low attenuation are compatible in the region.

4. Discussion

Interpretation and discussion of the analyses made constitute one of the most important points of the study. Compared to previous attenuation studies, although the results show slight differences in some regions, there are no contradictory results. The part of the discussion will be organized as southern Alaska, western Alaska, northern Alaska, and central Alaska.

4.1. Southern Alaska

High seismicity is seen in southern Alaska, which is under the control of the subduction zone formed by the subduction of the Pacific plate beneath the North American plate. The stress transfers resulting from the subduction zone, and the movements of the Pacific and North American plates are also the sources of extensive seismicity in the inner regions of Alaska (Jiang et al. 2018). Seismic events on the Pacific plate, where the Alaskan Gulf is located, occur at depths of less than 50 kilometers. In the subduction zone, in the northwest direction events occur more and more deeply from trench to back-arc (Wadati-Benioff Zone). The seismicity occurring at a depth of

approximately 100 kilometers in the forearc region reaches 150 kilometers in the back-arc region. This seismicity at intermediate depths also provides evidence for the existence of the subduction plate (Ratchkovski 2002). The reason for the lack of seismicity and volcanism in the Yakutat Terrane, located in the southeast is the fact that the Yakutat microplate is warmer and younger than the Pacific plate. In addition, it is anhydrous compared to the Pacific plate (Berg et al. 2020).

Attenuation, defined as an inverse of the quality factor (Q), is sensitive to temperature. Also, attenuation is partially insensitive to low partial melt or rock composition, unlike seismic velocities. In this way, it is useful as an imaging tool in subduction zones. These measurements, provided by attenuation, provide insights into where melting may take place (Stachnik, Abers, and Christensen 2004). Attenuation studies in the region (e.g., Soto Castaneda et al. 2021) correlate with the attenuation maps we have created. From the Cook Inlet with the lowest attenuation of the region (forearc) to Central Alaska, the attenuation represents the cold subduction slab. We obtained a higher attenuation value in the arc and back-arc regions. We think that the reason for this may be the effect of melt and volatile content on attenuation (Takei 2017), and we note it as a topic that we can investigate further for better understanding in the future.

4.2. Western Alaska

Unlike south and central Alaska, west Alaska is an area with relatively little seismic activity. The effect of the subduction zone, which is hundreds of kilometers southeast of the region, is relatively continuous. According to Curie

& Hyndman 2006, the effect of mantle temperatures extends hundreds of kilometers into the back-arc. It is an indication that the region has a warmer lithosphere-asthenosphere compared to other regions (Berg et al. 2020). These results are also consistent with the heat flow map of the region (Batir, Blackwell, and Richards 2016) (Fig 6). Intraplate seismicity features are more dominant in the region (Biswas et al. 1986). There is east-west compression by the Bering Strait in northwest Alaska. Additionally, according to Biswas et al. 1980, the tectonic mechanism of the region also controls regional magmatism. The region's relatively warm and shallow lithosphere-asthenosphere boundary and sparse geochemical and stress data indicate that the Bering Sea leads to this region (Berg et al. 2020). In conclusion, the high attenuation observed in this region is consistent with the areas of intracontinental magmatism and quaternary volcanism which is the Espenberg volcanic field located in the Seward Peninsula.

4.3. Northern Alaska

Unlike other parts of Alaska, North Alaska is an area with a cold and thick lithosphere (Gama et al. 2021). It is determined that Moho has a depth of 50 km and the lithosphere is up to 200 km thick under the Brooks Mountains (Ward and Lin 2018; Jiang et al. 2018). It is thought that the northward movement or mantle flow of the Yakut indentor controls this tectonic regime (Finzel et al. 2015). In addition, the intraplate deformation extends to the southern edge of the western Brooks Mountains and near the Eastern Brooks Mountains and Richardson Mountains (Jiang et al. 2018). In addition, in the Northeastern Brooks Mountains the lithosphere is weaker and deforms more rapidly in the south (Gaudreau et al. 2019). This deformed and relatively

higher temperature region explains the high attenuation seen in northeast Alaska in our attenuation results. These results are also consistent with the heat flow map of the region (Batir, Blackwell, and Richards 2016) (Fig 6). Additionally, the Colville Basin, located north of the Brooks Mountain range, is an undeformed and seismically inactive region with a thick cold lithosphere. The low attenuation we obtained in this region correlates well with the features of the region (Fig 7).

4.4. Central Alaska

The stresses created by the subduction zone in southern Alaska are seen for hundreds of kilometers up to the interior of Alaska where the deformation is accomplished by crustal seismicity. Many earthquakes are caused by the Denali fault in the south and the Kaltag and Tintina fault systems in the north, which are large-scale strike-slip faults (Ratchkovski 2002). In addition, the thinnest continental lithosphere (~60 km) (Gama et al. 2021), thinner crust, and a shallow Moho depth (~30 km) are observed under the Yukon Composite Terrane, which is between these faults (Ward and Lin 2018; Miller and Moresi 2018; Berg et al. 2020). However, it is also considered that crustal thickness and temperature in the central Alaska region increase north and east and reach maximum south of the Brooks Mountains (Jiang et al. 2018). This thin upper plate lithosphere continues into the Seward Peninsula in western Alaska. Subducting plate seismicity and upper plate magmatic activities show the role of subducting fluids and melts in this tectonic mechanism (Gama et al. 2021). These results are also consistent with the heat flow map of the region, especially on the north side of the Denali fault (Batir, Blackwell, and Richards 2016) (Fig 6). According to our

attenuation analysis results, except for the segment of the subduction slab that is north of the Denali fault (low attenuation, Δt*=~-0.07 s), the region generally shows moderate to high attenuation (Δt*=0-0.05 s). The very complex structural features of central Alaska cause the attenuation values in the region to differ (value of Δt* from -0.1 to 0.05 s). These different attenuations correlate well with our analysis results.

5. Conclusions

We created a teleseismic attenuation map with EarthScope Transportable Array (TA) and other broadband deployments in and around Alaska (Fig 2). Of the 370 events that met our criteria, we used 209 that passed our quality control test to create our map. Our Δt* estimates largely correlated well with our expectations, with some regional exceptions (Fig 3).

As one of the most seismically active regions of the world, Alaska exhibits a wide variety of structural features. The subduction zone, located in southern Alaska and formed by the subduction of the Pacific plate under the North American plate, is the source of tectonism in Alaska. Alaska's tectonism is controlled by intracontinental deformation.

Our results show the lowest attenuation (Δt*=-0.15 s) corresponds to the subduction slab in southern Alaska, and the highest attenuation (Δt*=0.15 s) is in the arc and back-arc region located northwest of the Cook Inlet basin. Results show high attenuation in western Alaska, especially around the Espenberg Volcanic field (Δt*= 0.04-0.1 s). In northern Alaska, the area north of the Brooks Mountains shows low attenuation (Δt*= 0- -0.1 s), but high attenuation (Δt*= 0.05-0.1 s) is seen around the Richardson Mountains in the

northeastern part of the area. This region shows seismicity occurs at the boundaries between high and low attenuation regions. In Central Alaska, except for the subduction slab (Δt^*= ~0.1 s), the region shows moderate-high attenuation (Δt^*= 0-0.05 s).

Our results are consistent with different structural regions such as subduction zone, arc, back-arc, foreland, quaternary volcanism, orogenetic structures, and basins. It also correlates well with properties such as seismicity, magmatism and deformation, and heat flow.

Figures

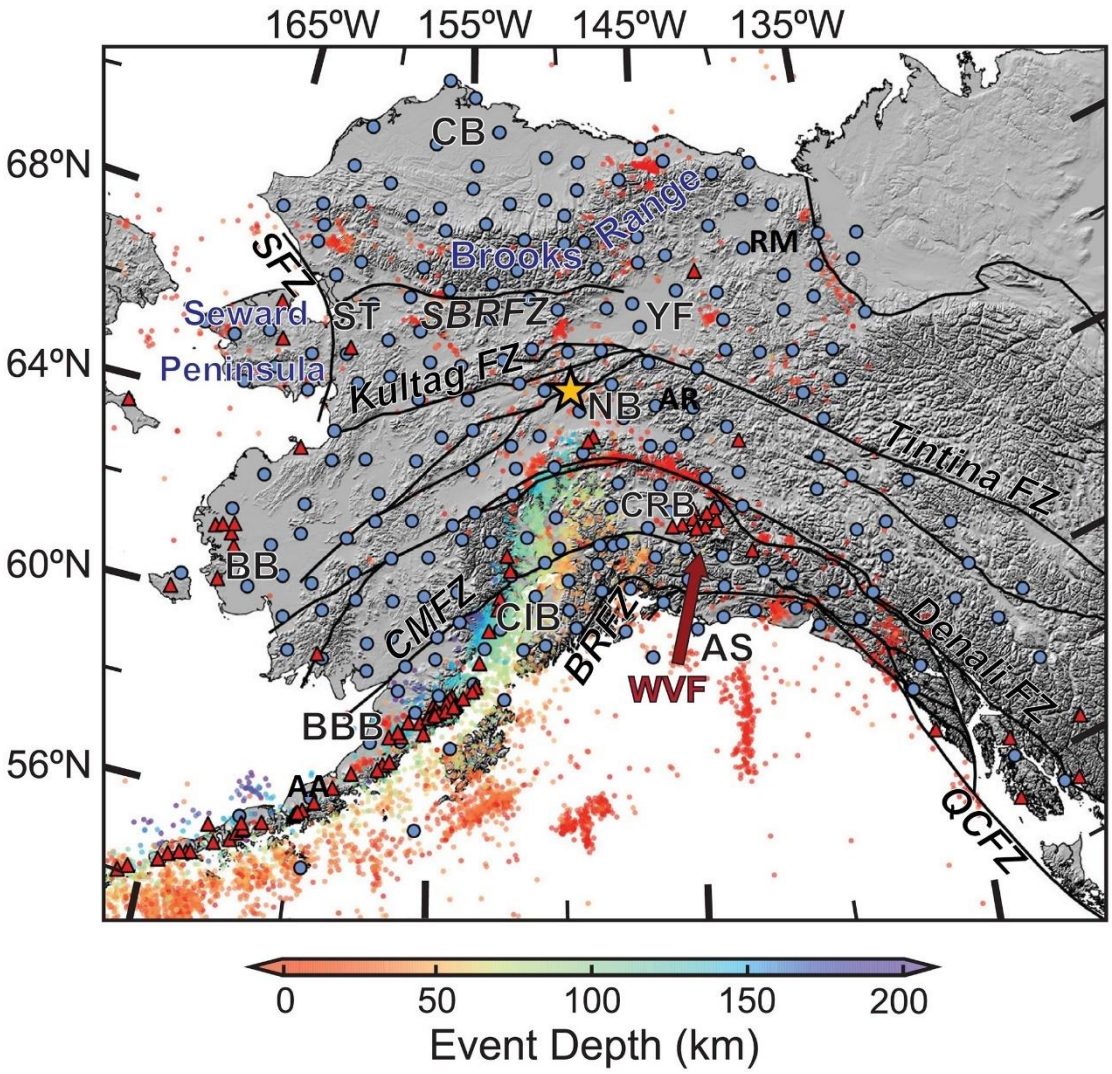

Figure 1. Map showing topography and earthquakes from 1980 to May 2019 with Mw > 4, shown as colored dots according to depth. Volcanoes (Holocene and Eocene) are marked as red triangles and Alaska Transportable Array stations. Important features are labeled on the map including fault zones (skewed and ending with “FZ”), basins (bold), and the Wrangell volcanic field (red, “WVF”). Fault zones include the Sevier, southern Brooks Range, Kultag, Tintina, Denali, Castle Mountain, border ranges, and queen Charlotte fault zones. Basins include Bethel Basin, Bristol Bay basin, Colville Basin, Copper River basin, cook Inlet Basin, Alaskan shelf, Nenana Basin, Selawik trough, Yukon flats, Richardson Mountain, Alaska Range, and Aleutian Range (Modified from Berg et al. 2020).

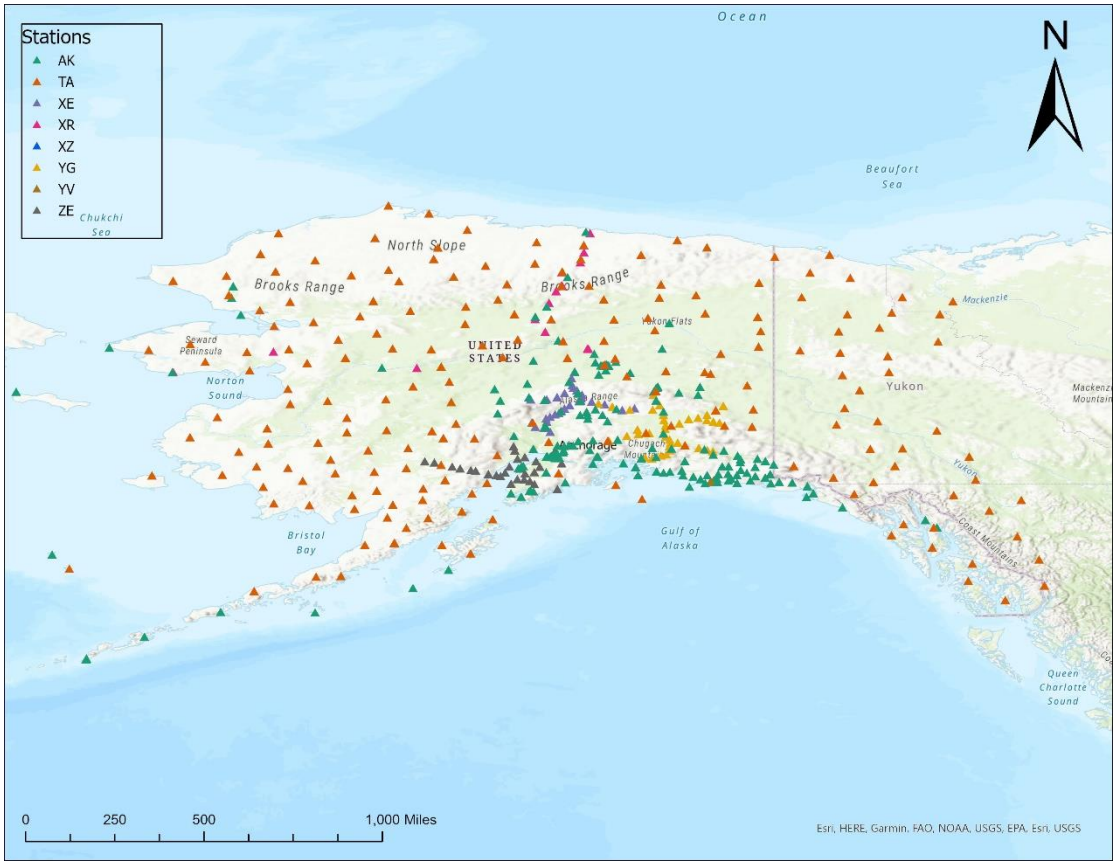

Figure 2. The map shows stations locations (triangles) used in the study.

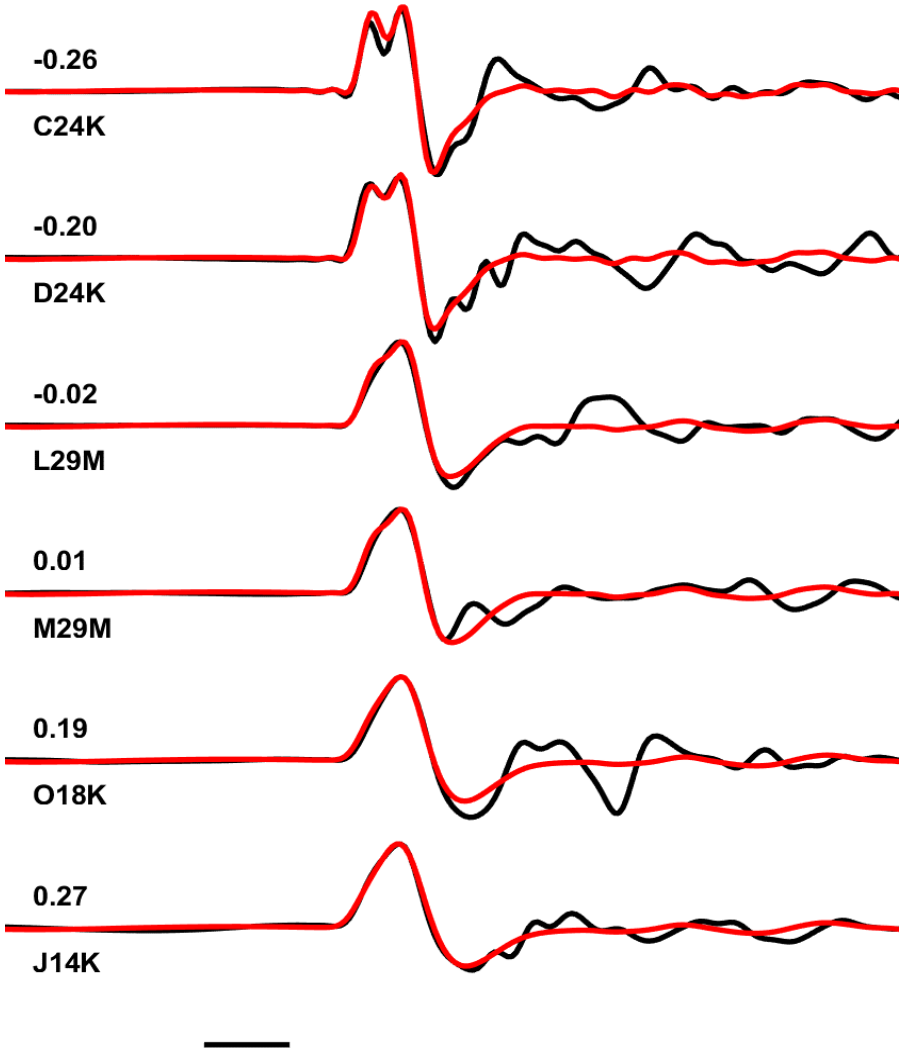

Figure 3. The measurements are done in the time domain, using a waveform-matching approach. Black lines – observed waveforms; red lines – synthetic waveforms. Δt* values and station names shown for each trace.

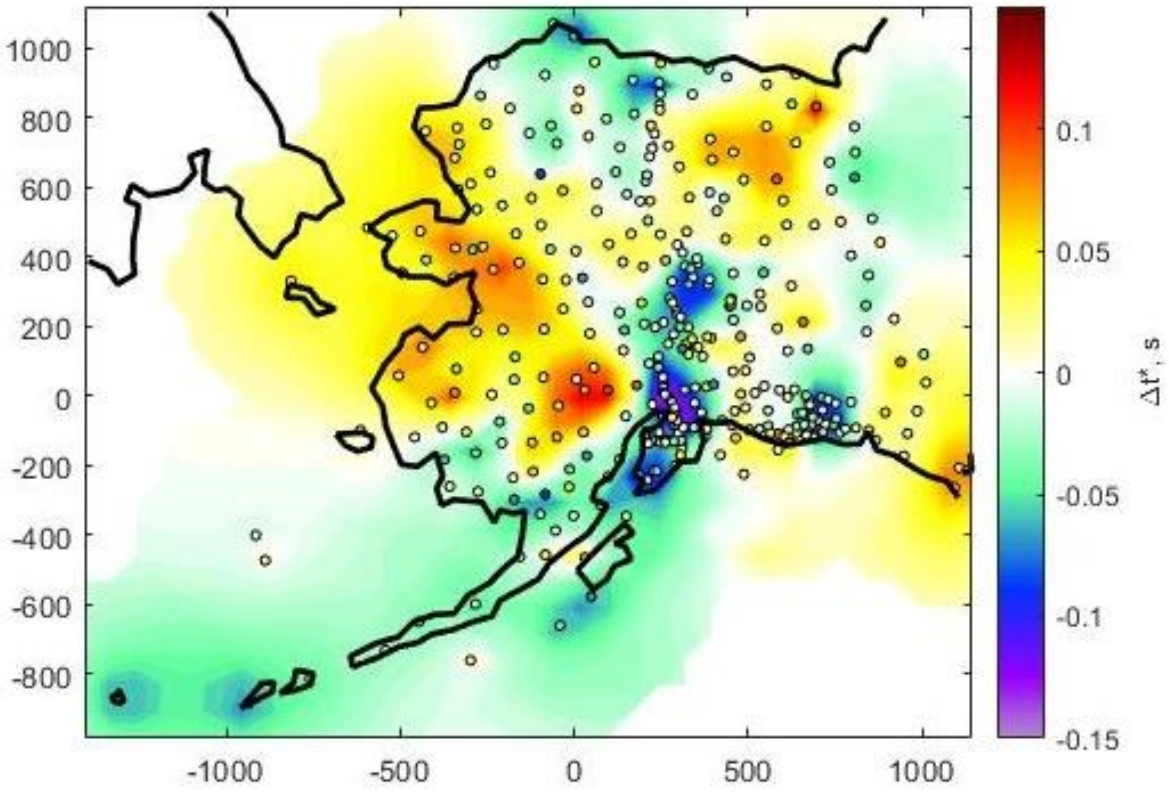

Figure 4. The map shows a Δt* result

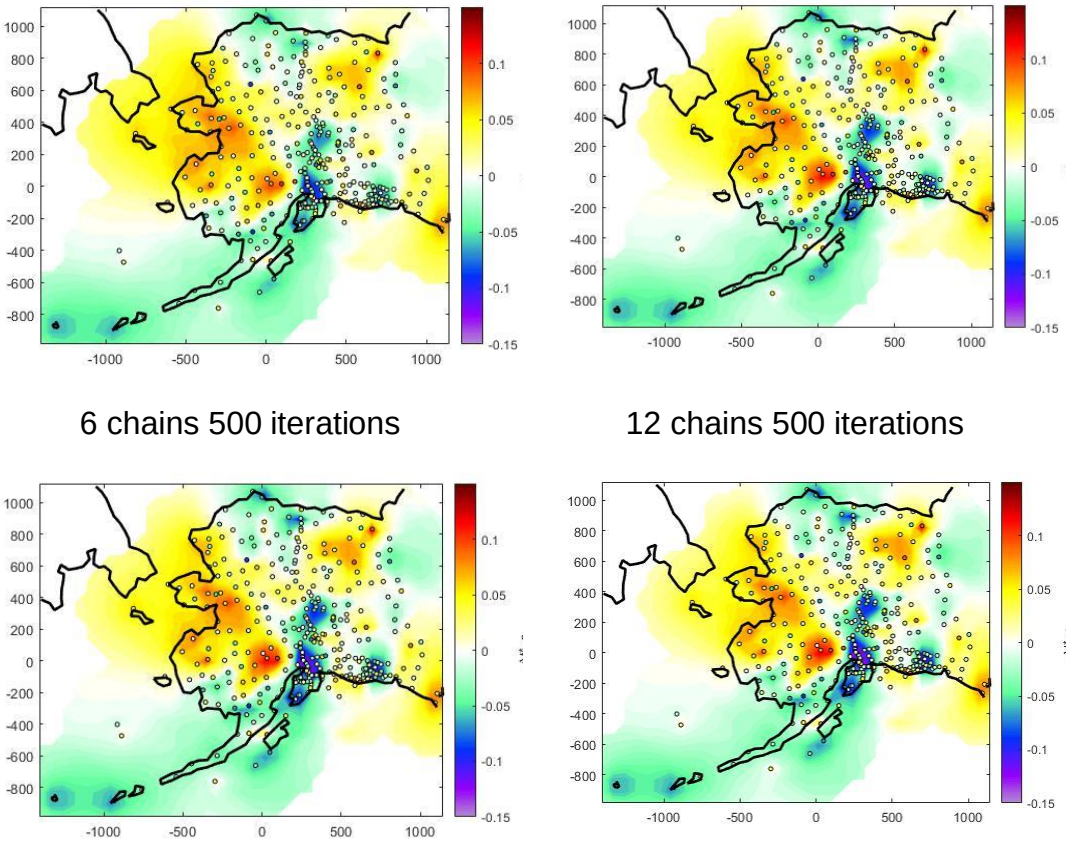

Figure 5. Different results for MCMC test

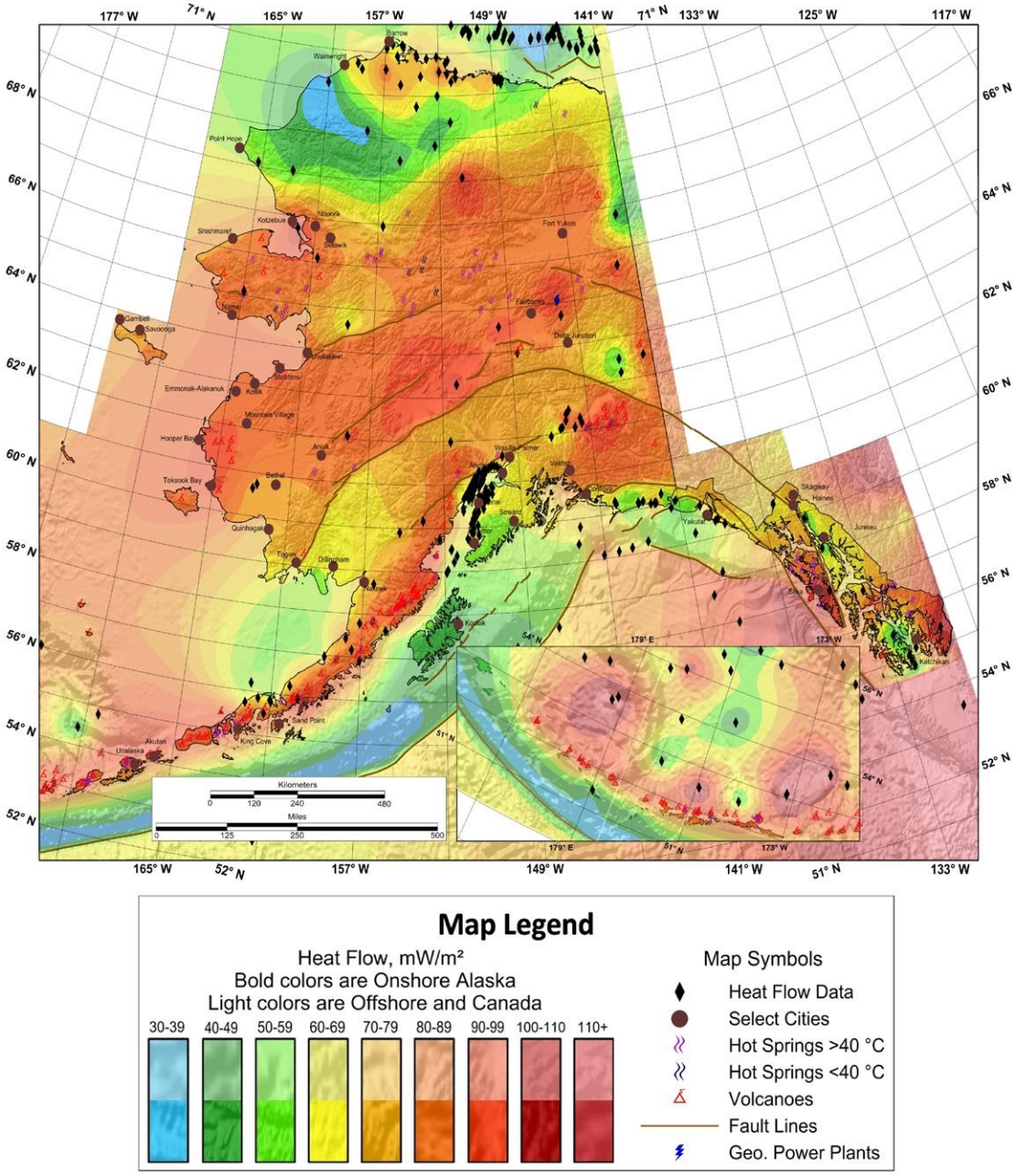

Figure 6. Heat flow map of Alaska. Two-tone coloring is used to emphasize onshore Alaska as bolder colors versus offshore and Canada that are opaque (From Batir, Blackwell, and Richards 2016).

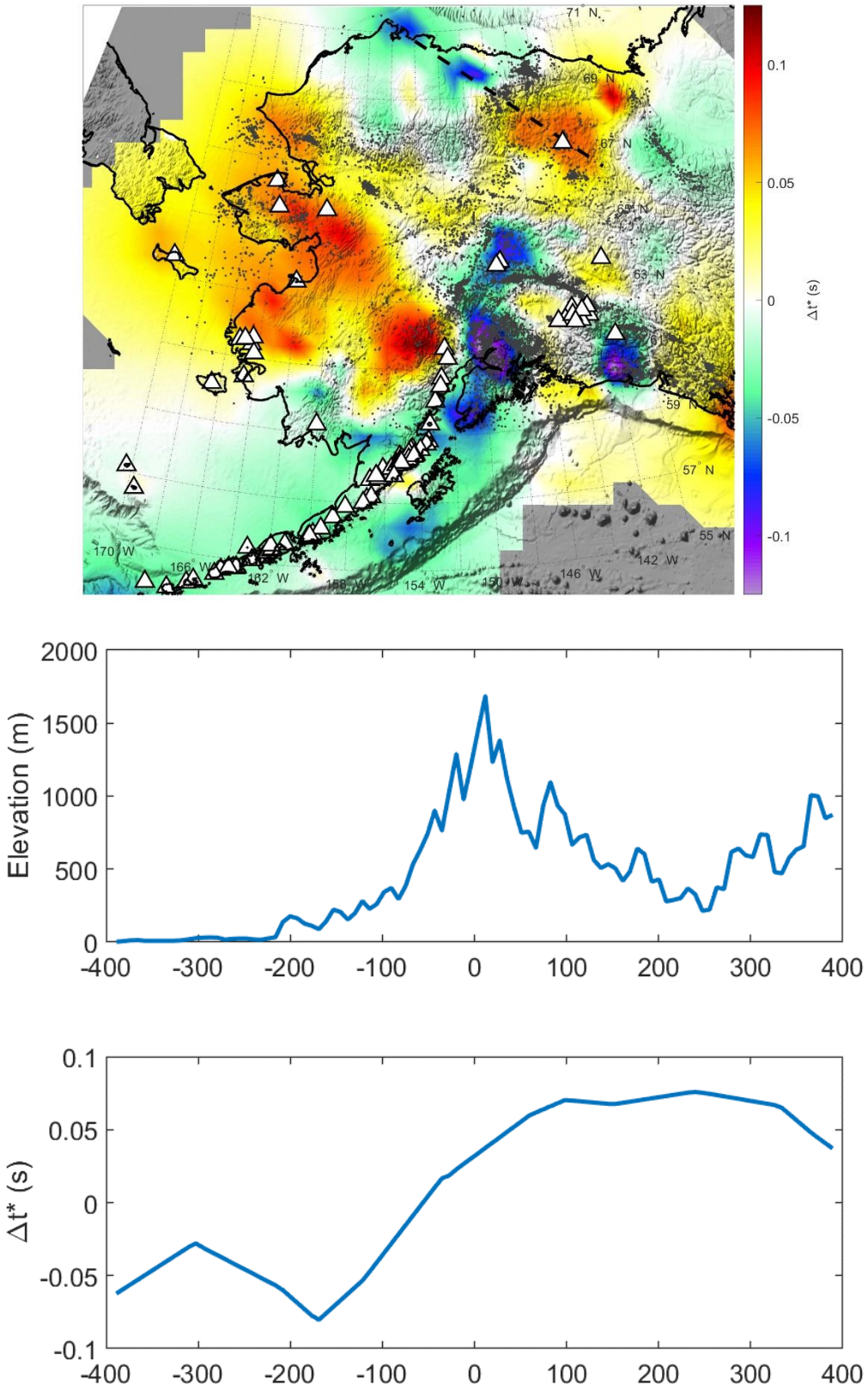

Figure 7. The map shows a Δt* result. Volcanos (white triangles), seismicity (gray dots) (above). Elevation and Δt* graph. The location of the profile is shown by the dashed line on the *Δ*t* map (below).

Bibliography

Alaska Earthquake Center, Univ. of Alaska Fairbanks. 1987. “Alaska Regional Network.” SEED data. International Federation of Digital Seismograph Networks. https://doi.org/10.7914/SN/AK

Bardsley, Johnathan M. 2012. “MCMC-Based Image Reconstruction with Uncertainty Quantification.” SIAM Journal on Scientific Computing 34 (3): A1316–32. https://doi.org/10.1137/11085760X

Batir, Joseph F, David D Blackwell, and Maria C Richards. 2016. “Heat Flow and Temperature-Depth Curves throughout Alaska: Finding Regions for Future Geothermal Exploration.” Journal of Geophysics and Engineering 13 (3): 366–78. https://doi.org/10.1088/1742-2132/13/3/366

Bemis, Sean P., and Wesley K. Wallace. 2007. “Neotectonic Framework of the North-Central Alaska Range Foothills,” January. https://doi.org/10.1130/2007.2431(21)

Berg, Elizabeth M., Fan-Chi Lin, Amir Allam, Vera Schulte-Pelkum, Kevin M. Ward, and Weisen Shen. 2020. “Shear Velocity Model of Alaska Via Joint Inversion of Rayleigh Wave Ellipticity, Phase Velocities, and Receiver Functions Across the Alaska Transportable Array.” Journal of Geophysical Research: Solid Earth 125 (2). https://doi.org/10.1029/2019JB018582

Bezada, Maximiliano J. 2017. “Insights into the Lithospheric Architecture of Iberia and Morocco from Teleseismic Body-Wave Attenuation.” Earth and Planetary Science Letters 478 (November): 14–26. https://doi.org/10.1016/j.epsl.2017.08.029

Biswas, N.N., J. Pujol, G. Tytgat, and K. Dean. 1986. “Synthesis of Seismicity Studies for Western Alaska.” Tectonophysics 131 (3–4): 369–92. https://doi.org/10.1016/0040-1951(86)90183-6

Byrnes, Joseph S., Maximiliano Bezada, Maureen D. Long, and Margaret H. Benoit. 2019. “Thin Lithosphere beneath the Central Appalachian Mountains: Constraints from Seismic Attenuation beneath the MAGIC Array.” Earth and Planetary Science Letters 519 (August): 297–307. https://doi.org/10.1016/j.epsl.2019.04.045

Byrnes, Joseph S., and Maximiliano Bezada. 2020. “Dynamic Upwelling Beneath the Salton Trough Imaged With Teleseismic Attenuation Tomography.” Journal of Geophysical Research: Solid Earth 125 (11). https://doi.org/10.1029/2020JB020347

Christensen, Douglas, and Geoff Abers. 2020. “Fate and Consequences of Yakutat Terrane Subduction beneath Eastern Alaska and the Wrangell Volcanic Field.” SEED data. International Federation of Digital Seismograph Networks. https://doi.org/10.7914/SN/YG_2016

Christensen, Douglas, Roger Hansen, and Geoff Abers. 1999. “Broadband Experiment Across the Alaska Range.” SEED data. International Federation of Digital Seismograph Networks. https://doi.org/10.7914/SN/XE_1999

Coakley, Bernard J., and Anthony B. Watts. 1991. “Tectonic Controls on the Development of Unconformities: The North Slope, Alaska.” Tectonics 10 (1): 101–30. https://doi.org/10.1029/90TC01982

Dixit, Nilesh C., and Catherine Hanks. 2021. “Basement Structure and Styles of Active Tectonic Deformation in Central Interior Alaska.” Geosciences 11 (3): 127. https://doi.org/10.3390/geosciences11030127

Eberhart-Phillips, Donna, Peter J. Haeussler, Jeffrey T. Freymueller, Arthur D. Frankel, Charles M. Rubin, Patricia Craw, Natalia A. Ratchkovski, et al. 2003. “The 2002 Denali Fault Earthquake, Alaska: A Large Magnitude, Slip-Partitioned Event.” Science 300 (5622): 1113–18. https://doi.org/10.1126/science.1082703

Finzel, Emily S., Lucy M. Flesch, Kenneth D. Ridgway, William E. Holt, and Attreyee Ghosh. 2015. “Surface Motions and Intraplate Continental Deformation in Alaska Driven by Mantle Flow.” Geophysical Research Letters 42 (11): 4350–58. https://doi.org/10.1002/2015GL063987

Gama, Isabella, Karen M. Fischer, Zachary Eilon, Hannah E. Krueger, Colleen A. Dalton, and Lucy M. Flesch. 2021. “Shear-Wave Velocity Structure beneath Alaska from a Bayesian Joint Inversion of Sp Receiver Functions and Rayleigh Wave Phase Velocities.” Earth and Planetary Science Letters 560 (April): 116785. https://doi.org/10.1016/j.epsl.2021.116785

Gao, S. 1997. “A Bayesian Nonlinear Inversion of Seismic Body-Wave Attenuation Factors.” Bulletin of the Seismological Society of America 87 (4): 961–70. https://doi.org/10.1785/BSSA0870040961

Gaudreau, É., E. K. Nissen, E. A. Bergman, H. M. Benz, F. Tan, and E. Karasözen. 2019. “The August 2018 Kaktovik Earthquakes: Active Tectonics in Northeastern Alaska Revealed With InSAR and Seismology.” Geophysical Research Letters 46 (24): 14412–20. https://doi.org/10.1029/2019GL085651

Gutenberg, Beno, and C. F. Richter. 1941. “Seismicity of the Earth.” In Geological Society of America Special Papers, 34:1–126. Geological Society of America. https://doi.org/10.1130/SPE34-p1

Hansen, Roger, and Gary Pavlis. 2005. “Collaborative Research: St. Elias Erosion/Tectonics Project.” SEED data. International Federation of Digital Seismograph Networks. https://doi.org/10.7914/SN/XZ_2005

IRIS Transportable Array. 2003. “USArray Transportable Array.” SEED data. International Federation of Digital Seismograph Networks. https://doi.org/10.7914/SN/TA

Jiang, Chengxin, Brandon Schmandt, Kevin M. Ward, Fan-Chi Lin, and Lindsay L. Worthington. 2018. “Upper Mantle Seismic Structure of Alaska From Rayleigh and S Wave Tomography.” Geophysical Research Letters 45 (19). https://doi.org/10.1029/2018GL079406

Koehler, R.D., G.A. Carver, and Alaska Seismic Hazards Safety Commission. 2018. “Active Faults and Seismic Hazards in Alaska.” MP 160. Alaska Division of Geological & Geophysical Surveys. https://doi.org/10.14509/29705

Lanza, Federica, Clifford H. Thurber, Ellen M. Syracuse, John A. Power, and Abhijit Ghosh. 2020. “Seismic Tomography of Compressional Wave Velocity and Attenuation Structure for Makushin Volcano, Alaska.” Journal of Volcanology and Geothermal Research 393 (March): 106804. https://doi.org/10.1016/j.jvolgeores.2020.106804

Miller, Meghan S., and Louis Moresi. 2018. “Mapping the Alaskan Moho.” Seismological Research Letters 89 (6): 2430–36. https://doi.org/10.1785/0220180222

Nayak, Avinash, Donna Eberhart-Phillips, Natalia A. Ruppert, Hongjian Fang, Melissa M. Moore, Carl Tape, Douglas H. Christensen, Geoffrey A. Abers, and Clifford H. Thurber. 2020. “3D Seismic Velocity Models for Alaska from Joint

Tomographic Inversion of Body-Wave and Surface-Wave Data." Seismological Research Letters 91 (6): 3106–19. https://doi.org/10.1785/0220200214

Ratchkovski, N. A. 2002. "New Constraints on Tectonics of Interior Alaska: Earthquake Locations, Source Mechanisms, and Stress Regime." Bulletin of the Seismological Society of America 92 (3): 998–1014. https://doi.org/10.1785/0120010182

Schmandt, Brandon, and Fan-Chi Lin. 2014. "P and S Wave Tomography of the Mantle beneath the United States." Geophysical Research Letters 41 (18): 6342–49. https://doi.org/10.1002/2014GL061231

Shearer, Peter M. 2009. Introduction to Seismology. 2nd ed. Cambridge: Cambridge University Press. https://doi.org/10.1017/CBO9780511841552

Skarlatoudis, Andreas A, Hong Kie Thio, and Paul G Somerville. 2022. "Estimating Shallow Shear-Wave Velocity Profiles in Alaska Using the Initial Portion of P Waves from Local Earthquakes." Earthquake Spectra 38 (2): 1076–1102. https://doi.org/10.1177/87552930211061589

Song, Xiaodong, and Douglas Christensen. 2010. "CSEDI: Observational and Theoretical Constraints on the Structure and Rotation of the Inner Core." SEED data. International Federation of Digital Seismograph Networks. https://doi.org/10.7914/SN/XR_2004

Soto Castaneda, R. A., G. A. Abers, Z. C. Eilon, and D. H. Christensen. 2021. "Teleseismic Attenuation, Temperature, and Melt of the Upper Mantle in the Alaska Subduction Zone." Journal of Geophysical Research: Solid Earth 126 (7). https://doi.org/10.1029/2021JB021653

Stachnik, Joshua C., Geoffrey A. Abers, and Douglas H. Christensen. 2004. "Seismic Attenuation and Mantle Wedge Temperatures in the Alaska Subduction Zone: BEAAR Q." Journal of Geophysical Research: Solid Earth 109 (B10). https://doi.org/10.1029/2004JB003018

Takei, Yasuko. 2017. "Effects of Partial Melting on Seismic Velocity and Attenuation: A New Insight from Experiments." Annual Review of Earth and Planetary Sciences 45 (1): 447–70. https://doi.org/10.1146/annurev-earth-063016-015820

Tape, Carl, Douglas H. Christensen, and Melissa M. Moore-Driskell. 2019. "Southern Alaska Lithosphere and Mantle Observation Network." SEED data. International Federation of Digital Seismograph Networks. https://doi.org/10.7914/SN/ZE_2015

Tian, You, and Dapeng Zhao. 2012. "Seismic Anisotropy and Heterogeneity in the Alaska Subduction Zone: Anisotropy and Heterogeneity in Alaska." Geophysical Journal International 190 (1): 629–49. https://doi.org/10.1111/j.1365-246X.2012.05512.x

Tisato, Nicola, Claudio Madonna, and Erik H. Saenger. 2021. "Attenuation of Seismic Waves in Partially Saturated Berea Sandstone as a Function of Frequency and Confining Pressure." Frontiers in Earth Science 9 (April): 641177. https://doi.org/10.3389/feart.2021.641177

Tommasi, A., A. Vauchez, and S. Neves. 2009. "Intraplate Deformation: The Role of Rheological Heterogeneity and Anisotropy of the Lithospheric Mantle (Invited)" 2009 (December): T41E-01.

Waite, Gregory. 2012. “Bering Glacier Surge Seismic Experiment.” SEED data. International Federation of Digital Seismograph Networks. https://doi.org/10.7914/SN/YV_2010

Wang, Yanbin, Lupei Zhu, Feng Shi, Alexandre Schubnel, Nadege Hilairet, Tony Yu, Mark Rivers, et al. 2017. “A Laboratory Nanoseismological Study on Deep-Focus Earthquake Micromechanics.” Science Advances 3 (7): e1601896. https://doi.org/10.1126/sciadv.1601896

Ward, Kevin M., and Fan-Chi Lin. 2018. “Lithospheric Structure Across the Alaskan Cordillera From the Joint Inversion of Surface Waves and Receiver Functions.” Journal of Geophysical Research: Solid Earth 123 (10): 8780–97. https://doi.org/10.1029/2018JB015967

Zhu, Zhao, Maximiliano J. Bezada, Joseph S. Byrnes, and Heather A. Ford. 2021. “Evidence for Stress Localization Caused by Lithospheric Heterogeneity From Seismic Attenuation.” Geochemistry, Geophysics, Geosystems 22 (11). https://doi.org/10.1029/2021GC009987